

Search for rare B meson decays at the *BABAR* experiment

R. Cheaib

On behalf of the *BABAR* collaboration

Department of Physics, University of Mississippi, 108 Lewis Hall, University MS 38677

E-mail: rachac@phys.olemiss.edu

Abstract. $\rightarrow s$ transitions are flavour-changing neutral current (FCNC) processes that play an important role in the search for physics beyond the Standard Model (SM). Contributions from virtual particles in the loop are predicted to deviate observables, such as the branching fraction, from their SM expectations. Using data from the BaBar experiment, we present the first search for the rare decay $B^+ \rightarrow K^+ \tau^+ \tau^-$. The *BABAR* results on the measurement of the angular asymmetries of $B \rightarrow K^* \ell^+ \ell^-$, where $\ell = e$ or μ , are also reported. In addition, using a time-dependent analysis of $B \rightarrow K_S^0 \pi^+ \pi^- \gamma$, the mixing induced CP-asymmetry for the radiative FCNC decay, $B \rightarrow K_S^0 \rho \gamma$, is measured, along with an amplitude analysis of the $m_{K\pi}$ and $m_{K\pi\pi}$ spectrum.

1. Introduction

$\rightarrow s$ transitions are highly suppressed in the SM and only occur via loop or box diagrams. Using an effective low-energy theory, the Lagrangian for $\rightarrow s$ transitions can be separated into two distinct parts: the long distance (low-energy) contributions contained in the operator matrix elements and the short-distance (high-energy) physics described by the Wilson coefficients. Measurements of such rare FCNC B meson decays are interesting since they can provide experimental constraints on the associated Wilson coefficients and are thus a stringent test of the SM. Furthermore, contributions from new-physics particles, like a charged Higgs [2], can deviate these Wilson coefficients or require the introduction of new operator matrix elements, and thus this is an interesting hunt for physics beyond the SM.

The *BABAR* experiment [3] collected 424 fb^{-1} of data [4] by colliding electrons and positrons at the center-of-mass (CM) energy of the $\Upsilon(4S)$ resonance. The $\Upsilon(4S)$ decays into $B\bar{B}$ pair, resulting in more than 479 million $B\bar{B}$ events to study and analyze. Using the full *BABAR* dataset, a measurement of the $B^+ \rightarrow K^+ \tau^+ \tau^-$ branching fraction [5], $B \rightarrow K^* \ell^+ \ell^-$ angular asymmetries [6] and $B \rightarrow K_S^0 \rho \gamma$ mixing-induced CP-asymmetry [7] is performed.

2. Branching fraction measurement of $B^+ \rightarrow K^+ \tau^+ \tau^-$

$B^+ \rightarrow K^+ \tau^+ \tau^-$ [8] is a FCNC process with a branching fraction in the range $1\text{--}2 \times 10^{-7}$ [9]. It is the third-lepton generation equivalent of $B \rightarrow K \ell^+ \ell^-$, where $\ell = e$ or μ . The large mass of the τ lepton may provide improved sensitivity to new-physics contributions as compared to its light lepton counterparts [10, 11]. For instance, in two-Higgs-doublet-models [2], the Higgs-lepton-lepton vertex is proportional to m_τ^2 and thus contributions to the total decay rate, as well as

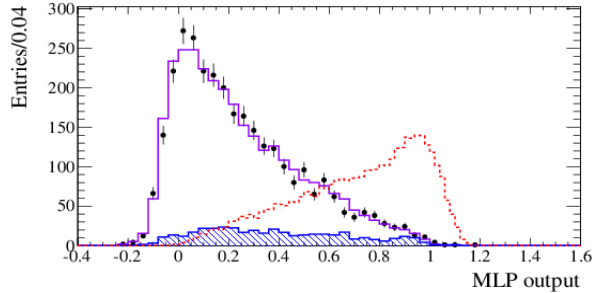


Figure 1. MLP output distribution for the $B^+ \rightarrow K^+ \tau^+ \tau^-$ analysis. The signal MC distribution is shown (dashed) with arbitrary normalization, along with the data (points) and the expected combinatorial (shaded) plus m_{ES} -peaking (solid) background contributions.

other observables, can be significant. The branching fraction of $B^+ \rightarrow K^+ \tau^+ \tau^-$ is measured by exclusively reconstructing one B meson, referred to as the B_{tag} , in the $\Upsilon(4S) \rightarrow B\bar{B}$ decay using hadronic modes, and then examining the rest of the event for the $B^+ \rightarrow K^+ \tau^+ \tau^-$ signal. This technique is referred to as the hadronic B_{tag} reconstruction, and is ideal for decays with missing energy. With exclusive reconstruction of the B_{tag} , the four-vector of the other B , the B_{sig} , can also be fully determined and thus the kinematics of the event are better constrained. The τ is required to decay only via leptonic modes: $\tau^- \rightarrow e^- \bar{\nu}_e \nu_\tau$ or $\tau^- \rightarrow \mu^- \bar{\nu}_\mu \nu_\tau$, and thus there are three possible final states: $e^+ e^-$, $\mu^+ \mu^-$ or $e^+ \mu^-$ with their associated neutrinos.

To select for $B^+ \rightarrow K^+ \tau^+ \tau^-$, every event is required to have exactly one properly-reconstructed charged B_{tag} with an energy substituted mass, m_{ES} , that lies within the range of the mass of a B meson. The m_{ES} of a B_{tag} candidate is given by $m_{\text{ES}} = \sqrt{E_{\text{CM}}^2 - \vec{p}_{B_{\text{tag}}}^2}$, where E_{CM} is half the total colliding energy and $\vec{p}_{B_{\text{tag}}}$ is the 3-momentum of the reconstructed B_{tag} , in the CM frame. Furthermore, $B^+ \rightarrow K^+ \tau^+ \tau^-$ events are required to have nonzero missing energy, which is calculated by subtracting all signal side tracks and clusters from the B_{sig} four-vector. A signal event is also required to have 3 tracks, one satisfying the particle identification (PID) criteria of a K and two of an electron or muon. In addition, the presence of massive τ leptons imposes an upper limit on the K momentum, which restricts the s_B distribution, given by $s_B = (p_{B_{\text{sig}}} - p_K)^2 / m_B^2$, of signal events to higher values as compared with background events. Therefore, a requirement of $s_B > 0.45$ is applied. At this point, the main source of background is from combinatorial events with semi-leptonic charmed B decays, such as $B \rightarrow D^{(*)} \ell \nu_\ell$, $D^{(*)} \rightarrow K \ell \nu_\ell$. To suppress this background, a multi-layer perceptron (MLP) neural network, consisting of eight discriminating variables such as the angle between the lepton and the oppositely charged kaon in the $\tau^+ \tau^-$ rest frame, is used. The neural network is then trained and tested for each of the three signal channels, and the combined MLP output is shown in Fig. 1. The final step in the signal selection is a requirement on the MLP output for each signal channel.

The data yield, after the MLP output cut, is determined separately for each of the three signal channels and then combined into one $B^+ \rightarrow K^+ \tau^+ \tau^-$ result. No significant excess is observed in the $e^+ e^-$ or $\mu^+ \mu^-$ channels, while a 3.7σ excess is observed in the $e^+ \mu^-$ channel. Examination of the input and output distributions of the $e^+ \mu^-$ channels does not show any clear evidence of signal-like behaviour or mis-modelling of the background. Furthermore, the combined excess for all three modes is less than 2σ . In the absence of signal, the combined upper limit at the 90% confidence level is measured to be $\mathcal{B}(B^+ \rightarrow K^+ \tau^+ \tau^-) < 2.6 \times 10^{-3}$. This is the first search for $B^+ \rightarrow K^+ \tau^+ \tau^-$.

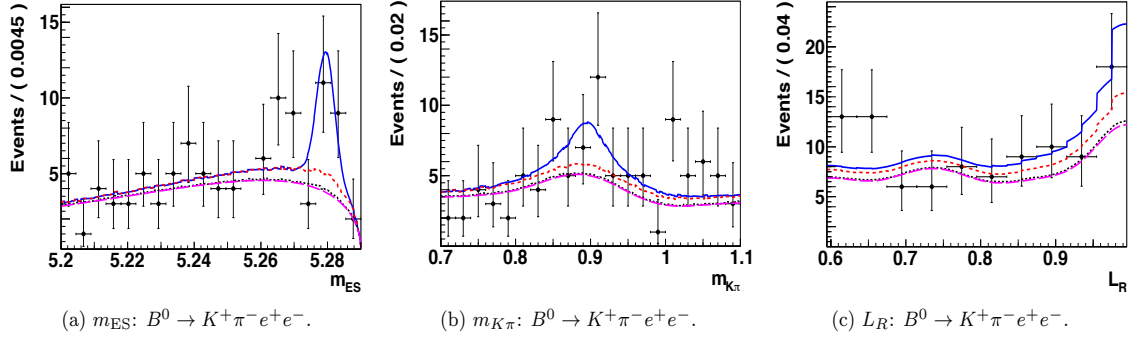


Figure 2. 3-D fit projections for $B^0 \rightarrow K^+ \pi^- e^+ e^-$ in q_5^2 . Each event class is shown: combinatorial (magenta long dash) and charmonium background events (black dots), crossfeed signal events (red short dash) and total pdf (solid blue).

3. Angular asymmetries in $B \rightarrow K^* \ell^+ \ell^-$

$B \rightarrow K^* \ell^+ \ell^-$ is also a FCNC process, with an amplitude expressed in terms of hadronic form factors and the C_7, C_9 , and C_{10} Wilson Coefficients[6]. The angular distributions of $B \rightarrow K^* \ell^+ \ell^-$, specifically the K^* longitudinal polarization, F_L , and the forward-backward asymmetry, A_{FB} , are notably sensitive to physics beyond the SM [12]-[13] and have been previously measured by various experiments [14]-[18].

For any given value of the q^2 , the kinematic distribution of the $B \rightarrow K^* \ell^+ \ell^-$ decay products can be expressed in terms of three distinct angles: θ_K , the angle between the K and the B in the K^* rest frame, θ_l , the angle between the lepton and the B in the $\ell^+ \ell^-$ rest frame, and ϕ , the angle between the $\ell^+ \ell^-$ and $K\pi$ decay planes in the B rest frame [6]. After integrating out ϕ and θ_l , F_L can be determined using a fit to $\cos \theta_K$ of the form $\frac{1}{\Gamma(q^2)} \frac{d\Gamma}{d(\cos \theta_K)} = \frac{3}{2} F_L(q^2) \cos^2 \theta_K + \frac{3}{4} (1 - F_L(q^2)) (1 - \cos^2 \theta_K)$. Similarly, A_{FB} can be extracted after integrating over ϕ and θ_K using a fit to θ_l of the form $\frac{1}{\Gamma(q^2)} \frac{d\Gamma}{d(\cos \theta_l)} = \frac{3}{4} F_L(q^2) (1 - \cos^2 \theta_l) + \frac{3}{8} (1 - F_L(q^2)) (1 + \cos^2 \theta_l) + A_{FB}(q^2) \cos \theta_l$ [19].

To measure F_L and A_{FB} , $B \rightarrow K^* \ell^+ \ell^-$ signal events are reconstructed in one of the following final states: $K^{*+} (\rightarrow K_S^0 \pi^+) \mu^+ \mu^-$, $K^{*0} (\rightarrow K^+ \pi^-) \mu^+ \mu^-$, $K^{*+} (\rightarrow K^+ \pi^0) e^+ e^-$, $K^{*+} (\rightarrow K_S^0 \pi^+) e^+ e^-$, $K^{*0} (\rightarrow K^+ \pi^-) e^+ e^-$. Each K^* candidate is required to have an invariant mass ranging between 0.72 and 1.10 GeV/c^2 , and is combined with a pair of leptons, each with an individual momenta greater than 0.3 GeV/c . The m_{ES} and ΔE of the resulting B candidate is then determined and used to separate between signal and background events. Here, $\Delta E = E_B^* - E_{CM}/2$, where E_B^* is the CM energy of the B and E_{CM} is total CM energy.

The main source of background is from semileptonic B and D decays, as well as continuum background events with random combinations of leptons. Eight bagged decision trees (BDT) are trained to suppress these $B\bar{B}$ and $q\bar{q}$ backgrounds and a final requirement on ΔE and L_R is applied at the end of the signal selection. Here, L_R is a likelihood ratio which uses the output of the $B\bar{B}$ BDT to determine how likely a given event is signal vs background.

To extract the angular observables, the q^2 spectrum is divided into five disjoint bins ($q_1 - q_5$) of varying size, and an additional bin q_0 , ranging between 1.0 and 6.0 GeV^2/c^4 . An initial unbinned maximum likelihood fit to the m_{ES} , $m(K\pi)$, and L_R spectrums is performed to fix the normalizations and shapes of all probability density functions (pdfs) dependent on these three variables. Then, for each mode and each q^2 bin, the 3-D likelihood fit is used to fix the normalizations of events with $m_{ES} > 5.27 \text{ GeV}/c^2$. Third, $\cos \theta_K$ is added as a fourth dimension

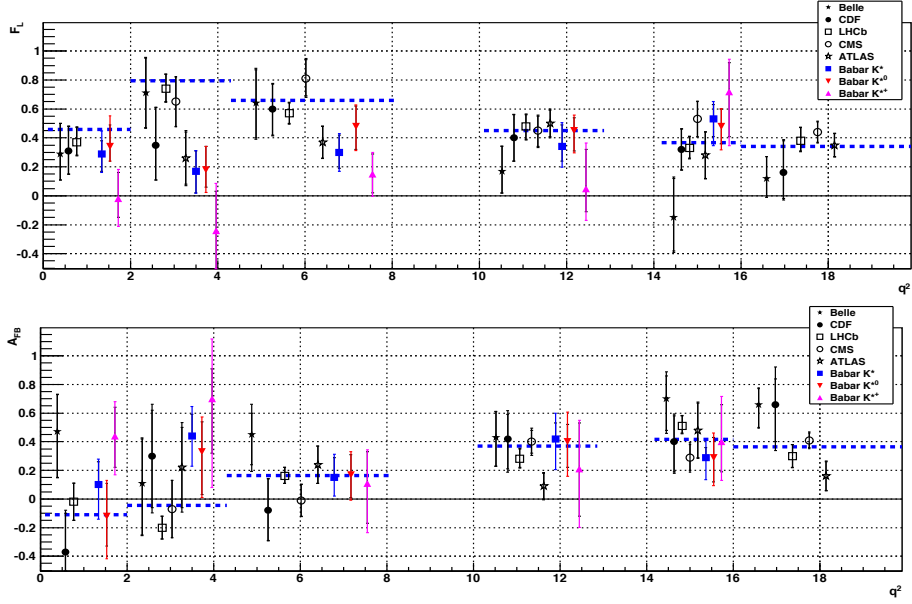


Figure 3. F_L and A_{FB} results for charged (magenta filled pointing-up triangle), neutral (red filled down-pointing triangle) and total $B \rightarrow K^* \ell^+ \ell^-$ (blue filled square) in disjoint q^2 bins. The SM expectations are shown as blue dashed lines along with results from other experiments: Belle [14] (black-filled star), CDF [15] (black-filled circle), LHCb [16] (black open square), CMS [17] (black open circle), and ATLAS [18] (black open star).

to the likelihood function, and four-dimensional likelihoods are defined for each signal mode and each q^2 bin with F_L as the only free parameter. Finally, the fitted value of F_L is then used as input to a similar 4-D fit, where $\cos \theta_l$ has been added as a fourth dimension instead of $\cos \theta_K$. The pdfs in the likelihood fit are defined for five different event classes: true signal events, crossfeed signal events, combinatorial backgrounds, backgrounds from charmonium decays, and finally backgrounds from hadronic decays which are only prominent for $\mu^+ \mu^-$ modes. Fig. 2 shows the initial 3-D fit projections for $B^0 \rightarrow K^+ \pi^- e^+ e^-$ in q^2_5 with the different event classes. F_L and A_{FB} are extracted in each q^2 bin for the charged, $B^+ \rightarrow K^{*+} \ell^+ \ell^-$, neutral, $B^0 \rightarrow K^{*0} \ell^+ \ell^-$, and total $B \rightarrow K^* \ell^+ \ell^-$ modes. The results are shown in Fig. 3 along with previous ones from Belle [14], CDF [15], LHCb [16], and CMS [17].

As can be readily seen, the $B^0 \rightarrow K^{*0} \ell^+ \ell^-$ results show good agreement with the SM expectations and other experiments. For the charged mode, the value of F_L is relatively small in the low q^2 region and thus exhibits tension with the SM expectation. An additional angular observable P_2 is defined such that $P_2 = (-2/3) \times A_{FB}/(1 - F_L)$. P_2 has diminished theoretical uncertainty and thus higher sensitivity to non-SM contributions. The tension at low q^2 is still found in the P_2 distribution and can be a hint of new physics, specifically the results are consistent with the existence of right-handed currents. This is the first measurement of angular asymmetries in $B^+ \rightarrow K^{*+} \ell^+ \ell^-$.

4. Mixing induced CP-asymmetry, S_{fCP} , in $B \rightarrow K_S^0 \rho \gamma$

In the SM, the photon emitted in $\rightarrow s \gamma$ transitions is predominantly left-handed, with contamination from right-handed photons suppressed by a factor of m_s/m_b [20]. This implies that B^0 (\bar{B}^0) mesons decay predominantly to right-handed (left-handed) photons and the mixing-induced CP-asymmetry in $B \rightarrow f_{CP} \gamma$ decays is expected to be small. However, various

new physics models [21, 22] introduce enhanced contributions from right-handed photons and thus alter the prediction of a small CP-asymmetry.

In this analysis, the mixing-induced CP-asymmetry of $B^0 \rightarrow K_S^0 \rho \gamma$, $S_{K_S^0 \rho \gamma}$, is measured using a time-dependent analysis of $B^0 \rightarrow K_S^0 \pi^+ \pi^- \gamma$. Due to the large natural width of the ρ meson, there is an irreducible contribution from the non-CP eigenstate $B^0 \rightarrow K^{*\pm} (\rightarrow K_S^0 \pi^\pm) \pi^\mp \gamma$ which affects $S_{K_S^0 \rho \gamma}$, and thus a dilution factor, $D_{K_S^0 \rho \gamma} \equiv S_{K_S^0 \pi^+ \pi^- \gamma} / S_{K_S^0 \rho \gamma}$, must be determined. Here, $S_{K_S^0 \pi^+ \pi^- \gamma}$ is the effective value of the mixing-induced CP asymmetry for the full $B^0 \rightarrow K_S^0 \pi^+ \pi^- \gamma$ dataset. To determine $D_{K_S^0 \rho \gamma}$, an amplitude analysis of the $m_{K\pi}$ spectra must be performed. Given the small number of events expected in the $B^0 \rightarrow K_S^0 \pi^+ \pi^- \gamma$ sample, the amplitudes of the resonant modes are determined from the charged $B^+ \rightarrow K^+ \pi^+ \pi^- \gamma$ mode instead and then extracted, under the assumption of isospin asymmetry, to the neutral mode. Furthermore, because the decay to the $K^+ \pi^+ \pi^- \gamma$ final state proceeds in general through three-body resonances first which then further decay into their $K^* \pi$ or $K \rho$ components, it is necessary to determine the three-body resonance content of the $m_{K\pi\pi}$ spectrum as well.

$B^+ \rightarrow K^+ \pi^+ \pi^- \gamma$ events are reconstructed from one high energy photon with $1.5 < E_\gamma < 3.5$ GeV, two oppositely-charged pions, and one charged kaon. These are combined to form a B candidate, whose m_{ES} should lie with 5.20 and 5.92 GeV/ c^2 and $|\Delta E| < 0.200$ GeV. A Fisher discriminant, consisting of six discriminating variables, is trained to suppress continuum background events. Furthermore, to reduce backgrounds from photons that originate from π^0 or η decay, a likelihood ratio, L_R , is constructed. To extract the $B^+ \rightarrow K^+ \pi^+ \pi^- \gamma$ yield, an unbinned extended maximum likelihood fit to the m_{ES} , ΔE , and Fisher discriminant output F is performed. The resulting branching fraction is measured to be $\mathcal{B}(B^+ \rightarrow K^+ \pi^+ \pi^- \gamma) = (24.5 \pm 0.9 \pm 1.2) \times 10^{-6}$.

The $m_{K\pi\pi}$ spectrum is then extracted from the maximum likelihood fit, and modeled as the coherent sum of five kaonic Breit-Wigner resonances: $K_1(1270)$, $K_1(1400)$, $K^*(1410)$, $K^*(1680)$ and $K_2^*(1430)$. The fit fraction of each resonance is determined and its corresponding branching fraction, given by $\mathcal{B}(B^+ \rightarrow K_{\text{res}} (\rightarrow K^+ \pi^+ \pi^-) \gamma)$, is computed. Furthermore, a binned maximum likelihood fit is further performed to the efficiency-corrected $m_{K\pi}$ spectrum. Using the phase space decay of the three-body resonances $m_{K\pi\pi}$, an efficiency map is determined and applied to the $m_{K\pi}$ spectrum. The latter is modeled as the projection of two 1^- P-wave components, $K^*(892)$ and $\rho(770)$, and one 0^+ S-wave component, $(K\pi)_0^{(*)}$. The branching fractions $\mathcal{B}(B^+ \rightarrow K_{\text{res}} \pi^+ \gamma)$ are also determined. Many of the measured branching fractions in this analysis are the first to be done or more accurate than previous world averages. Using the results of the $m_{K\pi}$ spectrum, the dilution factor is computed and yields $D_{K_S^0 \rho \gamma} = -0.78_{-0.17}^{+0.19}$.

To measure the time-dependent CP asymmetry, the proper-time difference, given by $\Delta t = t_{\text{rec}} - t_{\text{tag}}$, is determined, between a fully reconstructed $B^0 \rightarrow K_S^0 \rho \gamma$ decay (B_{rec}^0) and the other B in the event B_{tag} , which is partially reconstructed. The distance between the decay-vertex positions of B_{tag} and B_{rec} is measured and transformed to ΔE using the boost, $\beta\gamma = 0.561$, of the e^+e^- beams. To reconstruct the B_{tag} , a B -flavor tagging algorithm [23] is used, which combines various event variables to achieve optimal separation between the two B candidates in a signal event. $B^0 \rightarrow K_S^0 \pi^+ \pi^- \gamma$ events are reconstructed using the same signal selection as $B^+ \rightarrow K^+ \pi^+ \pi^- \gamma$, but with $K_S^0 \rightarrow \pi^+ \pi^-$. An unbinned maximum likelihood fit is then performed to the m_{ES} , ΔE , Fisher discriminant output, Δt and $\sigma_{\Delta t}$ distributions to extract the signal yield. The fit is shown in Fig 4 and yields a branching fraction $\mathcal{B}(B^0 \rightarrow K^0 \pi^+ \pi^- \gamma) = (20.5 \pm 2.0_{-2.2}^{+2.6}) \times 10^{-6}$. The CP-violation parameter is then determined to be $S_{K_S^0 \pi^+ \pi^- \gamma} = 0.14 \pm 0.25 \pm 0.03$. Using the calculated dilution factor and assuming isospin asymmetry, the resulting time-dependent CP asymmetry for $B^0 \rightarrow K_S^0 \rho \gamma$ is calculated to be: $S_{K_S^0 \rho \gamma} = -0.18 \pm 0.32_{-0.05}^{+0.06}$. This measurement is in agreement with previously published results [24]-[26] and shows no deviation from the SM prediction.

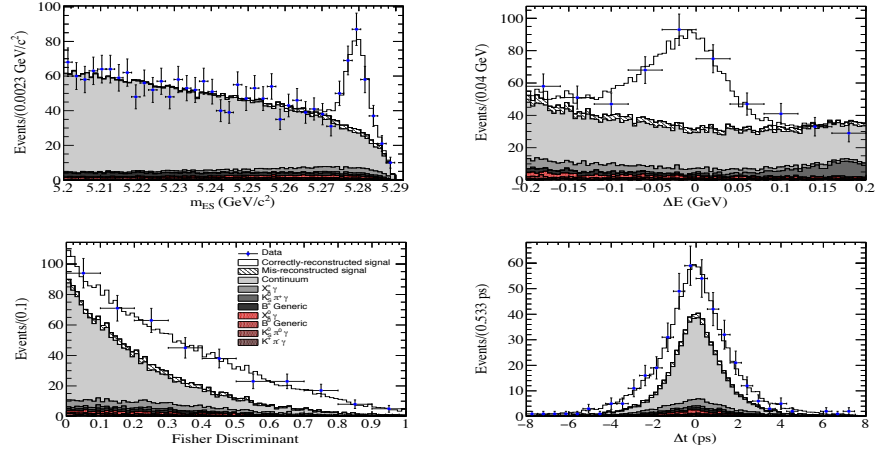


Figure 4. Distributions of m_{ES} (top left), ΔE , Fisher discriminant output F , and Δt with the fit results for the $B^0 \rightarrow K_S^0 \pi^+ \pi^- \gamma$ data sample. The data is shown as points with error bars and the stacked histograms represent the different background contributions.

5. Conclusion

Various interesting and leading results are still being produced using the *BABAR* dataset. An upper limit on the $B^+ \rightarrow K^+ \tau^+ \tau^-$ has been done for the first time. Furthermore, the angular asymmetries of $B \rightarrow K^* \ell^+ \ell^-$ are measured and display tension with the SM expectations in the low q^2 region. In addition, the time-dependent CP-asymmetry in $B \rightarrow K_S^0 \rho \gamma$ has been measured and shows consistency with the SM. $\rightarrow s$ transitions continue to be a promising probe of physics beyond the SM and a point of interest for current and future *B*-factories.

- [1] A. J. Bevan *et al.* [*BABAR* and Belle Collaborations], *Eur. Phys. J. C* **74**, 3026 (2014).
- [2] T. M. Aliev, M. Savci and A. Ozpineci, *J. Phys. G* **24**, 49 (1998).
- [3] B. Aubert *et al.* [*BABAR* Collaboration], *Nucl. Instrum. Meth. A* **729**, 615 (2013).
- [4] J. P. Lees *et al.* [*BABAR* Collaboration], *Nucl. Instrum. Meth. A* **726**, 203 (2013).
- [5] J. P. Lees *et al.* [*BABAR* Collaboration], arXiv:1605.09637
- [6] J. P. Lees *et al.* [*BABAR* Collaboration], *Phys. Rev. D* **93**, 052015 (2016).
- [7] J. P. Lees *et al.* [*BABAR* Collaboration], *Phys. Rev. D* **93**, 052013 (2016).
- [8] The charge conjugate mode $B^- \rightarrow K^- \tau^+ \tau^-$ is also implied.
- [9] C. Bouchard, G. P. Lepage, C. Monahan, H. Na and J. Shigemitsu, *Phys. Rev. Lett.* **111**, 162002 (2013).
- [10] Q. Yan *et al.*, *Phys. Rev. D* **62**, 094023 (2000).
- [11] D. Guetta and E. Nardi, *Phys. Rev. D* **58**, 012001 (1998).
- [12] T. Feldmann and J. Matias, *JHEP* **0301**, 074 (2003).
- [13] Y. G. Xu, R. M. Wang and Y.D. Yang, *Phys. Rev. D* **74**, 114019 (2006).
- [14] J. T. Wei *et al.* [*Belle* Collaboration], *Phys. Rev. Lett.* **103**, 171801 (2009).
- [15] T. Aaltonen *et al.* [*CDF* Collaboration], *Phys. Rev. Lett.* **108**, 081807 (2012).
- [16] R. Aaij *et al.* [*LHCb* Collaboration], *JHEP* **1308**, 131 (2013).
- [17] S. Chatrchyan *et al.* [*CMS* collaboration], *Phys. Lett. B* **727**, 77 (2013).
- [18] G. Aad *et al.* [*ATLAS* Collaboration], ATLAS-CONF-2013-038.
- [19] F. Kruger and J. Matias, *Phys. Rev. D* **71**, 094009 (2005).
- [20] D. Atwood, M. Gronau and A. Soni, *Phys. Rev. Lett.* **79**, 185 (1997).
- [21] K. Fujikawa and A. Yamada, *Phys. Rev. D* **49**, 5890 (1994).
- [22] P. L. Cho and M. Misiak, *Phys. Rev. D* **49**, 5894 (1994).
- [23] B. Aubert *et al.* [*BABAR* Collaboration], *Phys. Rev. Lett.* **99**, 171803 (2007).
- [24] J. Li *et al.* [*Belle* Collaboration], *Phys. Rev. Lett.* **101**, 251601 (2008).
- [25] B. Aubert *et al.* [*BABAR* Collaboration], *Phys. Rev. D* **78**, 071101 (2008).
- [26] Y. Ushiroda *et al.* [*Belle* Collaboration], *Phys. Rev. D* **74**, 111104 (2006).